

# Simulation of time-domain terahertz ellipsometry measurements towards data extraction

**Shane Smith, Pieter Neethling, Erich Rohwer**

Department of Physics, Stellenbosch University, Stellenbosch, South Africa

E-mail: [srsmith@sun.ac.za](mailto:srsmith@sun.ac.za)

**Abstract.** Terahertz time-domain transmission spectroscopy is a powerful tool for performing non-destructive spectroscopy on many materials. One known limitation of this spectroscopy technique is that it is not well suited for use with optically dense materials, such as aqueous solutions. One method to circumvent this limitation is by working in reflection, as opposed to transmission. In order to avoid alignment complications introduced by changing between a reference mirror and sample, as is required for standard specular reflection spectroscopy, ellipsometry can also be implemented which avoids the need for a reference. In our lab we have constructed a terahertz time-domain ellipsometer. In order to test data extraction techniques for the constructed setup, simulated measurements were generated to test the constraints of the setup. These simulated measurements can be used to construct data extraction algorithms for future measurements. It is found that the simulated data matches the experimental data, and thus the simulated data can be used for testing data extraction techniques developed for our setup.

## 1. Introduction

Terahertz (THz) radiation is a powerful tool for performing non-destructive spectroscopy on many materials. Most commercial and reported systems operate in transmission [1–3], but this does not allow for the examination of optically dense materials, such as aqueous solutions [4]. One method for circumventing such limitations is to work in reflection. This can be problematic, since it introduces alignment errors, due to changes between the sample and a reference mirror being required [5]. The alignment tolerance between the sample and mirror is experimentally challenging ( $< 1 \mu\text{m}$  positional accuracy) [5]. In our lab we have implemented ellipsometry to avoid the need for a reference, since this technique compares the s- and p-polarized light reflected from a sample in order to obtain information about the sample [6]. A custom designed time-domain THz ellipsometer has been constructed in our laboratory and is operational. In order to test the validity of the measurements as well as the extracted material parameters, experimental measurements are simulated. Material parameters can then be extracted from the simulated data, thereby testing the extraction model for accuracy.

Several steps are required to generate the expected THz time-domain electric field. This process is depicted by the flow diagram in figure 1. First an initial THz time-domain electric field,  $E_0$ , is generated. This field is then transformed to the frequency domain via a Fast Fourier Transform (FFT). The dielectric medium is represented by frequency domain transfer functions for both the p- and s-polarizations. These transfer functions contain the material properties of interest namely the frequency dependent refractive index and extinction coefficient.

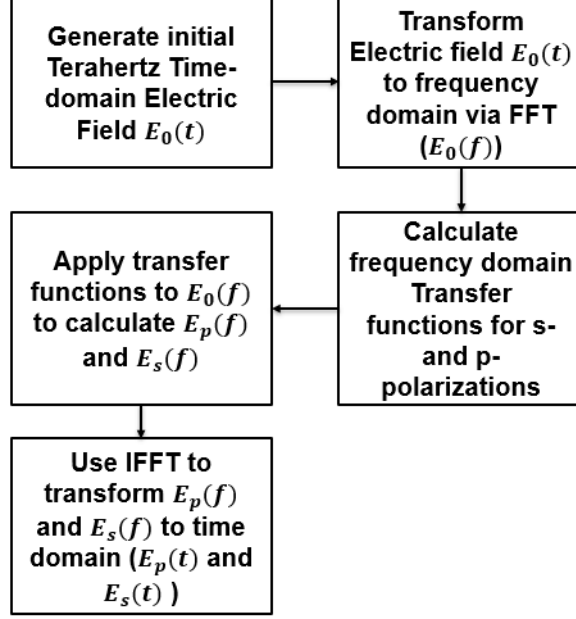


**Figure 1.** Flow diagram of the simulation process illustrating that all calculations occur in the frequency domain and measurements in the time domain.

Multiplication of the incident electric field with the transfer functions yields the expected detected signals (p and s) in the frequency domain. These two signals are then Fourier transformed to the time-domain, in order to represent the measured signals.

## 2. Incident THz time-domain electric field

In our setup we make use of photo-conductive antennae to generate THz radiation. Photo-conductive antennae are dipole antennae that are printed on photo-conductive substrates with short excitation lifetimes. Femtosecond laser pulses are used to optically trigger these antennae. When triggered, these antennae allow for a single electric current oscillation, which leads to the generation of THz electric fields. The electric field generated by the photo-conductive antenna can be described by the following equation [7]:

$$E(r, t) = \frac{l_e}{4\pi\epsilon_0 c^2 r} \frac{\partial J(t)}{\partial t} \sin \theta \quad (1)$$

$$J(t) = \frac{e\tau_s}{m} E_{DC} I_{opt}^0 \int_0^\infty e^{-(t-t')^2/\tau_p^2 - t'/\tau_c} [1 - e^{-t'/\tau_s}] dt' \quad (2)$$

where  $J(t)$  is the current in the dipole,  $l_e$  the effective length of the dipole,  $r$  is the distance between the emitting and receiving antennae and  $\theta$  the polar observation angle for the dipole. For the purposes of this simulation,  $\theta$  is taken to be  $90^\circ$ , since the optical path is perpendicular to the emitter. The carrier lifetime of the substrate is represented by  $\tau_c$ ,  $\tau_s$  is the momentum relaxation time of the substrate,  $m$  is the effective mass of the charge carriers,  $e$  is the charge of an electron and  $E_{DC}$  is the applied bias field. A Gaussian pump pulse with a temporal width, FWHM,  $\tau_p$  and intensity of  $I_{opt}^0$  is used [7].

Our pump pulse has a width (FWHM) of 90 fs, the substrate on which the antennae are printed has an excitation lifetime of 300 fs (in our setup we use low temperature grown GaAs as

the substrate), the momentum relaxation time is 25 fs,  $l_e$  is  $20\ \mu\text{m}$  and  $r$  is 45 mm (the distance between the emitter and the first collimation optic in our setup). The electric field represented by figure 2 is generated via equation 1.

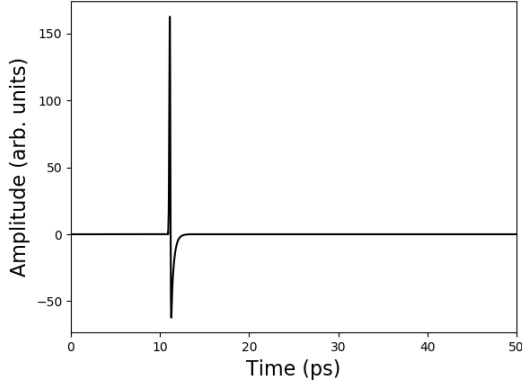


**Figure 2.** Time-domain electric field generated via equation 1 for a  $20\ \mu\text{m}$  antenna on low temperature grown GaAs.

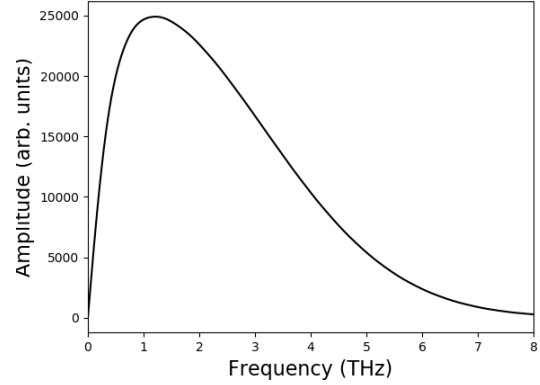


**Figure 3.** Frequency-domain electric field generated by performing an FFT on the electric field displayed in figure 2.

These values were chosen, since they correspond to the system in our laboratory [7].

It is easier to calculate the transfer functions for a sample in the frequency domain. In order to transform the THz electric field to the frequency domain a FFT is used. The FFT amplitude data for figure 2 is represented by figure 3.

### 3. Material transfer functions

In our simulation we will consider a single layer dielectric medium. According to the Fresnel equations, at the interface between two media with different refractive indexes, part of an incident electric field will be reflected and part will be transmitted.

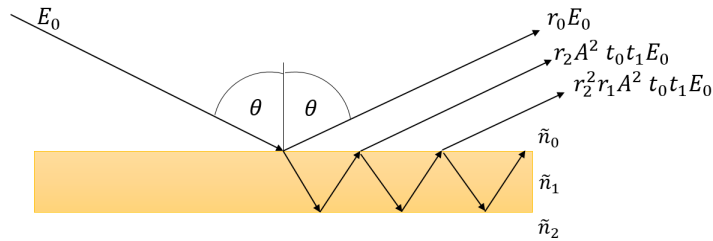


**Figure 4.** A diagram depicting the light-matter interaction for a single-layered dielectric sample.

Using Snell's laws the angle of transmission can be calculated and it is known that the angle of reflection is the same as the angle of incidence. According to the Lorentz model, as light travels through a medium, it undergoes both absorption and retardation [8]. In the case of a single layer dielectric medium, both external and internal reflections occur in the medium. A

depiction of this process can be seen in figure 4. Considering a material with refractive index  $n(f)$ , extinction coefficient  $k(f)$  and thickness  $d_0$ , we can calculate the expected reflected s- and p-polarized electric fields as follows:

$$E_s(t) = r_{s0}E_{s0}(t) + t_{s0}r_{s2}t_{s1}X^2E_{s0}(t - 2\tau) + t_{s0}r_{s2}^2r_{s1}t_{s1}X^4E_{s0}(t - 4\tau) + \dots \quad (3)$$

$$= r_{s0}E_{s0}(t) + t_{s0}r_{s2}t_{s1} \sum_{j=0}^{\infty} (r_{s1}r_{s2}X^2)^j E_{s0}(t - (j+1)2\tau) \quad (4)$$

$$E_p(t) = r_{p0}E_{p0}(t) + t_{p0}r_{p2}t_{p1}X^2E_{p0}(t - 2\tau) + t_{p0}r_{p2}^2r_{p1}t_{p1}X^4E_{p0}(t - 4\tau) + \dots \quad (5)$$

$$= r_{p0}E_{p0}(t) + t_{p0}r_{p2}t_{p1} \sum_{j=0}^{\infty} (r_{p1}r_{p2}X^2)^j E_{p0}(t - (j+1)2\tau) \quad (6)$$

$$\tau = \frac{dn}{c} \quad (7)$$

$$X = e^{\frac{-2\pi fkd}{c}} \quad (8)$$

$$d = \frac{d_0}{\cos \theta_1} \quad (9)$$

$$\theta_1 = \sin^{-1} \left( \frac{\tilde{n}_0}{\tilde{n}_1} \sin \theta_0 \right) \quad (10)$$

where  $t_{s0}$ ,  $t_{p0}$ ,  $r_{s0}$ ,  $r_{p0}$  are the transmission and reflection coefficients for the interface between the initial medium and the sample. The transmission and reflection coefficients for the interface between the sample and the initial medium are represented by  $t_{s1}$ ,  $t_{p1}$ ,  $r_{s1}$ ,  $r_{p1}$  and  $t_{s2}$ ,  $t_{p2}$ ,  $r_{s2}$ ,  $r_{p2}$  represent the transmission and reflection coefficients for the interface between the sample and the medium following the sample. These coefficients are calculated using the Fresnel equations. The attenuation and retardation coefficients,  $X$  and  $\tau$ , are as described by the Lorentz model [8]. The distance that the electric field travels through the medium is represented by  $d$ . The complex refractive indexes of the initial medium, the sample and the medium following the sample are represented by  $\tilde{n}_0$ ,  $\tilde{n}_1$  and  $\tilde{n}_2$ .

Due to the complex refractive index being frequency dependent, it is preferable to work in the frequency domain. Working in the frequency domain also allows for the transfer function associated with the medium to be separated from the electric field. To achieve this, a Fourier transform is performed on the electric fields

$$E_s(f) = (r_{s0}(f) + t_{s0}r_{s2}t_{s1}A \sum_{j=0}^{\infty} (r_{s1}r_{s2}A^2)^j) E_{s0}(f) \quad (11)$$

$$E_p(f) = (r_{p0}(f) + t_{p0}r_{p2}t_{p1}A \sum_{j=0}^{\infty} (r_{p1}r_{p2}A^2)^j) E_{p0}(f) \quad (12)$$

$$A = e^{\frac{-2\pi fkd}{c}} e^{\frac{-2i\pi fnd}{c}} = e^{\frac{-2i\pi f\tilde{n}d}{c}} \quad (13)$$

#### 4. Simulated THz electric field

Using equation 11 and 12 it is now possible to simulate a THz electric field for a dielectric sample. As an example, if we take a sample that has a flat real refractive index of 3.4177, a flat absorption coefficient of  $0.03 \text{ cm}^{-1}$  and a thickness of  $500 \mu\text{m}$ , that is surrounded by air, the following electric fields in the frequency domain are generated

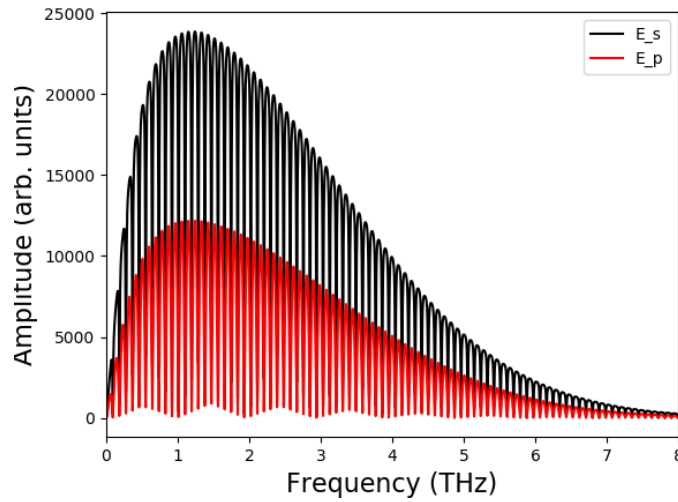


**Figure 5.** Frequency-domain electric fields generated by equations and for a sample with real refractive index  $3.4177$ , absorption coefficient  $0.03 \text{ cm}^{-1}$  and thickness  $500 \mu\text{m}$ .

These values are based on the characteristics of high resistivity silicon [9, 10].

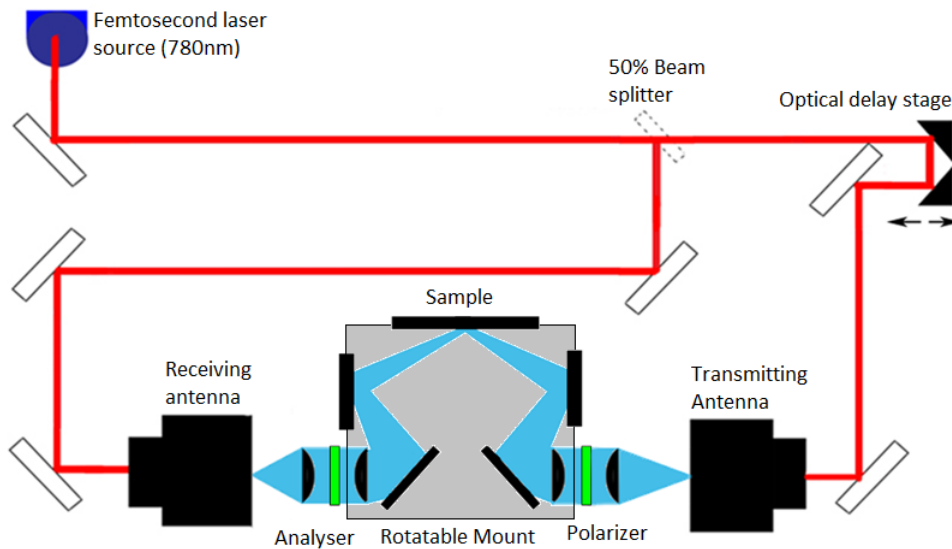


**Figure 6.** A diagrammatic representation of the experimental setup used by our lab.

By using an IFFT the electric fields can be transformed back to the time-domain. Experimental data for this sample was measured using a setup with a layout as depicted in figure 6. Since the experimental setup performs its measurements in the time-domain, it is convenient to compare the simulated data and experimental data in the time-domain.

By comparing figure 7 and 8, it is found that the simulated data correlates with the experimental data. The time delay between successive pulses correspond and, the phase shifts in pulses are as expected in both the simulated and experimental data (seen in pulses

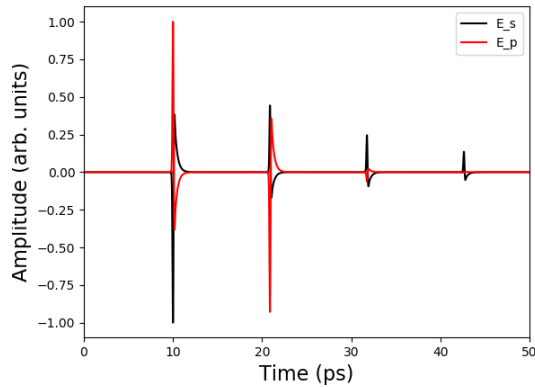


**Figure 7.** Normalized time-domain electric fields generated by taking an IFFT of electric fields presented in figure 5.

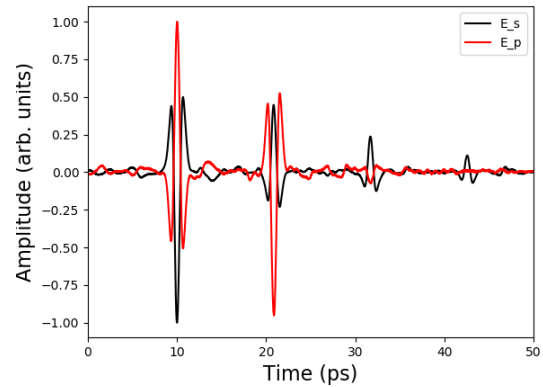


**Figure 8.** Normalized time-domain electric fields measured in our lab for a high resistivity silicon sample.

flipping when a  $\pi$  phase-shift occurs). Finally, the decrease in amplitude between successive pulses is also well matched.

## 5. Conclusion

The applicability of time-domain THz ellipsometry relies heavily on the quality of the material parameters that can be extracted from experimental data. In order to verify extracted material parameters, we have successfully simulated real time-domain THz ellipsometry measurements on high resistivity single crystalline Silicon, and compared these simulations to experimental measurements. The simulations and measurements agreed in shape and structure, which lends credibility to the simulated data. This simulated data will in future be used to test our material parameter extraction algorithms, in order to verify their accuracy. This verification is crucial in validating material parameters extracted from our experimental measurements of unknown or complex samples

## References

- [1] Pedersen J and Keiding S 1992 *IEEE Journal of Quantum Electronics* **28** 2518–2522
- [2] He M, Azad A K, Ye S and Zhang W 2006 *Optics Communications* **259** 389 – 392
- [3] Lenz M, Matheisen C, Nagel M and Knoch J 2017 *Applied Physics Letters* **110** 072103
- [4] Wu Y 2018 *Proc.SPIE* **10616** 10616 – 10616 – 9
- [5] Nagashima T and Hangyo M 2001 *Applied Physics Letters* **74** 3917–3919
- [6] Tompkins H and Irene E 2005 *Handbook of Ellipsometry* (William Andrew Publishing)
- [7] Sakai K 2005 *Terahertz Optoelectronics* 1st ed (Springer-Verlag New York, LLC, 233 Spring Street, New York, NY 10013, USA: Springer-Verlag)
- [8] Born M and Wolf E 1975 *Principles of Optics* 5th ed (Pergamon Press)
- [9] Li J and Li J 2008 *Microwave and Optical Technology Letters* **50** 1143–1146
- [10] Jepsen P 2007 *Optics Express* **15** 14717 – 14737